PNAS RESEARCH ARTICLE | NEUROSCIENCE

Peptidergic modulation of motor neuron output via CART signaling at C bouton synapses

Panagiotis E. Eleftheriadis[a,1], Konstantinos Pothakos[a,1], Simon A. Sharples[b], Panagiota E. Apostolou[a], Maria Mina[a], Efstathia Tetringa[a], Eirini Tsape[a], Gareth B. Miles[b], and Laskaro Zagoraiou[a,2]

Edited by Sten Grillner, Karolinska Institutet, Stockholm, Sweden; received January 17, 2023; accepted July 17, 2023

The intensity of muscle contraction, and therefore movement vigor, needs to be adaptable to enable complex motor behaviors. This can be achieved by adjusting the properties of motor neurons, which form the final common pathway for all motor output from the central nervous system. Here, we identify roles for a neuropeptide, cocaine- and amphetamine-regulated transcript (CART), in the control of movement vigor. We reveal distinct but parallel mechanisms by which CART and acetylcholine, both released at C bouton synapses on motor neurons, selectively amplify the output of subtypes of motor neurons that are recruited during intense movement. We find that mice with broad genetic deletion of CART or selective elimination of acetylcholine from C boutons exhibit deficits in behavioral tasks that require higher levels of motor output. Overall, these data uncover spinal modulatory mechanisms that control movement vigor to support movements that require a high degree of muscle force.

motor control | acetylcholine | cocaine and amphetamine regulated transcript | spinal cord | C boutons

Significance

A fundamental aspect of the control of movement is the ability to readily adjust the vigor of muscle contractions. Here, we describe a signaling pathway in the spinal cord that enhances the output of motor neurons, which activate muscles to produce movements. This pathway is mediated by a peptide encoded by the Cocaine-and-Amphetamine-Regulated-Transcript (CART). We show that CART is present, along with acetylcholine, in C bouton synapses located on motor neurons that are important for generating vigorous movements. We reveal that CART and acetylcholine facilitate motor neuron output through distinct, but parallel mechanisms. These findings provide insights into the cellular mechanisms that control movement and highlight pathways that could be targeted for the treatment of injuries and diseases affecting movement.

The generation of complex motor behavior is critically dependent on the ability to precisely time the sequence of muscle activation and to regulate the amount of force produced by muscles. Whilst the timing of muscle activation is largely encoded by integrated populations of spinal interneurons (1, 2), the strength of muscle activation, and subsequent movement vigor, is determined by motor neuron output. Importantly, motor neuron output is constantly adjusted to suit the task-dependent demands of diverse motor behaviors. These adjustments are often achieved by regulating cellular properties that determine motor neuron recruitment and firing rates (FR) (3–5). A range of neuromodulatory pathways, originating from higher centers and local interneurons, are responsible for this regulation of motor neuron properties. For example, descending sources of brainstem-derived monoamines amplify motor neuron firing by facilitating persistent inward currents (6–10). One of the most prominent spinally derived neuromodulatory pathways for the regulation of motor output is mediated by spinal V0c interneurons and their C bouton synapses at motor neurons (11, 12).

The broad V0 population of spinal interneurons, which are identified based on the expression of the Developing Brain Homeobox 1 transcription factor (Dbx1), was one of the first developmentally defined populations shown to provide direct input to motor neurons (13). The V0 population is composed of dorsal and ventral subpopulations (14, 15). The ventral subpopulation includes a small subset that can be identified based on the expression of the Paired-like homeodomain transcription factor 2 (Pitx2), which is further subdivided into cholinergic (V0c) and glutamatergic (V0g) subsets (12). Although V0c interneurons comprise only 2.5% of the cardinal V0 population, they represent the sole source of large cholinergic C bouton synapses at the soma and proximal dendrites of motor neurons. V0c interneurons, and their C boutons, support the key function of increasing motor output during tasks of increased motor demand (12). Although significant knowledge exists regarding the pre- and postsynaptic machinery of the C bouton synapse, the mechanisms by which this system adjusts motor output remain to be fully resolved. The traditional view is that the release of acetylcholine from C boutons increases motor neuron FR through the activation of postsynaptic M2 muscarinic receptors leading to downstream effects on a range of ion channels including calcium-activated potassium channels and Kv2.1 channels (12, 16).

Here, we reveal unique mechanisms by which V0c interneurons, and their C bouton synapses, regulate motor neuron activity. We show that a poorly understood signaling neuropeptide, the cocaine- and amphetamine-regulated transcript (CART), is expressed in V0c interneurons at all levels of the spinal cord and in most C boutons. Functional analysis reveals distinct yet parallel mechanisms for CART and acetylcholine in the amplification of the output of a subset of motor neurons, fast motor neurons, that are typically

Author contributions: G.B.M. and L.Z. designed research; P.E.E., K.P., S.A.S., P.E.A., M.M., E. Tetringa, E. Tsape, and L.Z. performed research; P.E.E., K.P., S.A.S., P.E.A., M.M., E. Tetringa, E. Tsape, and L.Z. analyzed data; G.B.M. and L.Z. supervised the project; and P.E.E., K.P., S.A.S., G.B.M., and L.Z. wrote the paper.

The authors declare no competing interest.

This article is a PNAS Direct Submission.

[1]P.E.E. and K.P. contributed equally to this work.

[2]To whom correspondence may be addressed. Email: lzagoraiou@bioacademy.gr.

This article contains supporting information online at https://www.pnas.org/lookup/suppl/doi:10.1073/pnas.2300348120/-/DCSupplemental.

Published September 21, 2023.

engaged only during tasks that require high levels of motor output (17). We found that CART facilitates the recruitment of fast but not slow motor neurons, whereas cholinergic pathways increase FR of fast motor neurons. Intriguingly, neither CART nor acetylcholine are critical for the formation or maintenance of C bouton synapse structure, but they are important for the generation of motor behaviors that require high levels of motor output. Together, these findings support that CART represents a parallel signaling mechanism at this important neuromodulatory synapse. Given that cholinergic modulation of output neurons is a common feature of neural networks throughout the CNS (18–20), our results are likely to be applicable to a range of networks and behaviors.

Results

CART Is Enriched in a Subset of Pitx2+ Spinal Interneurons. With the aim to identify markers to distinguish homogeneous, functionally defined subsets of interneurons involved in motor control and locomotion, we have previously performed a microarray screen (12) comparing the mRNA expression in the ventral and dorsal parts of the lumbar spinal cord of mice at postnatal day 8 (P8; Fig. 1*A*). We focused on genes that are preferentially expressed in the ventral, lumbar spinal cord where locomotor circuits reside (21). This screen resulted in the identification of 82 genes that were expressed more than three-fold higher in the ventral compared to the dorsal horn (12) two of which, Pitx2 and Short-stature homeobox 2, have been previously described and are expressed exclusively in the subsets of spinal interneurons that play key roles in the control of motor neuron excitability and locomotor rhythm generation, respectively (12, 22). This study focuses on one of the genes highlighted by our screen, the *Cart* gene, one of the most enriched transcripts in the ventral spinal cord, which encodes a signaling peptide called CART that, following in situ hybridization, was revealed to be expressed in a small interneuron subset in the intermediate zone of the spinal cord. CART was found to be expressed in a 3.4:1 ratio in the ventral compared to the dorsal horn. *Cart* mRNA expression in P8 mice was detected in neurons located near the central canal, in the motor neuron area (Laminae VIII and IX), and the dorsal horn of the cervical (Fig. 1*B*), thoracic (Fig. 1*C*), and lumbar (Fig. 1 *D* and *E*) segments of the spinal cord. In addition, *Cart*-expressing neurons were also detected in the intermediate zone of the thoracic spinal cord, representing sympathetic preganglionic neurons (SPNs) (*SI Appendix*, Fig. S1), consistent with previous reports (23–25). A similar expression profile was observed in the adult thoracic spinal cord (P25), where *Cart* mRNA was observed near the central canal, in the motor neuron area, in putative SPNs, and in the dorsal horn (Fig. 1*F*).

We next performed immunohistochemistry experiments to examine the distribution of the CART peptide within the spinal cord. Consistent with in situ hybridization, CART-labeled somata were identified near the central canal, in the motor neuron area, in regions where SPNs reside, and in the dorsal horn of the P8 upper lumbar spinal cord (Fig. 1*G*). CART-expressing neurons, as revealed by immunohistochemistry, recapitulated the in situ hybridization data in all spinal segments. Interestingly, we not only detected CART immunoreactivity in somata but also in fibers in the superficial dorsal horn, Laminae VII-X, and through the anterior white commissure. A similar distribution of CART expression was also observed in spinal cords obtained from mice at P0 suggesting that CART expression is also present at birth, albeit with a lower intensity in the superficial dorsal horn (Fig. 1*H*).

We next set out to determine the identity of CART-expressing neurons found near the central canal. Our attention was drawn to clusters of CART+ neurons located lateral to the central canal, that appear at all spinal levels and were reminiscent of the V0cg (Pitx2+) subsets of interneurons. As shown in Zagoraiou et al. (12), the Pitx2 transcription factor defines two small interneuron subsets of the V0 population, the cholinergic V0c and the glutamatergic V0g, located in clusters close to the central canal and forming columns running throughout the rostrocaudal axis. The cholinergic V0c subset is known to be the sole source of cholinergic C bouton synapses on the somata and proximal dendrites of motor neurons. Therefore, should Pitx2 and CART expression colocalize, a new marker and more importantly a potential neurotransmitter for the V0cg interneurons may be at hand.

To test this hypothesis, we crossed a *Pitx2::Cre* (26) mouse line with a *Rosa.lsl.tdTomato* (27) reporter line to express the fluorescent protein tdTomato in the tissues after excision of the LoxP-flanked stop cassette by Cre recombinase. CART was expressed in a subset of tdTomato-expressing somata (81%) (Fig. 1 *I–Iii* and *J–Jiii*), suggesting the CART peptide may only be expressed in a subset of Pitx2+ interneurons. Surprisingly, 99% of V0c interneurons, colabeled with choline acetyltransferase (ChAT) and tdTomato, were CART+, specifically 98% in cervical, 99% in thoracic, and 100% in upper lumbar levels (Fig. 1 *K–Kiv*). On the other hand, CART was only found in 65% of tdTomato+ ChAT– V0g interneurons; 64% in the cervical, 73% in thoracic, and 57% in lumbar segments. Additionally, a second microarray screen was performed, further supporting our findings. mRNA expression was compared between Pitx2+ interneurons and neighboring V2a Sox14+ interneurons, revealing CART mRNA 37.5 times enriched in the Pitx2+ population compared to the Sox14+ one.

CART Is Localized in C Bouton Synapses. V0c interneurons give rise to large cholinergic synapses called C boutons that are located on the somata and proximal dendrites of alpha motor neurons and are important for facilitating output during tasks that require greater motor output (12). We therefore next examined CART expression at C boutons to determine whether CART might be a novel signaling peptide at this synapse. Immunohistochemistry for CART demonstrated a high density of CART+ puncta in lamina VIII and IX. We also detected some CART+ motor neuron somata (ChAT+), as previously detected in the in situ hybridization experiments (Fig. 2 *A–Aii* and *SI Appendix*, Fig. S2). Focusing on lamina IX, the CART+ puncta were found to colocalize with ChAT+ terminals on motor neurons of P8 (Fig. 2 *B–Bii*) and P25 mice (Fig. 2 *C–Cii*), suggesting that CART may serve as a second neurotransmitter at C bouton synapses. A heterogenous distribution of CART immunoreactivity was observed within the C bouton synapses (*SI Appendix*, *Supplementary results* and Figs. S3 and S4), summarized in Table 1. Interestingly, other synapses on motor neurons such as 5HT (descending inputs), vGluT1 (sensory), and vGluT2 (mainly spinal excitatory) present very low colocalization percentages with CART (*SI Appendix*, Fig. S5). Specifically, we find that only 3.1% of vGluT1, 0.6% of the vGluT2, and 1.5% of the 5HT synapses contain CART.

Parallel Amplification of Motor Neuron Output by CART and Acetylcholine. We next sought to investigate whether CART provides an additional, physiologically relevant signaling mechanism at C bouton synapses. Given that C boutons are potent modulators of motor neuron excitability (16, 28), we assessed whether CART could modulate the excitability of spinal motor neurons. We also compared any effects of CART with those of muscarine, which activates the predominant, known acetylcholine-based signaling mechanisms at C bouton synapses. We examined the effect of CART and muscarine on motor neuron

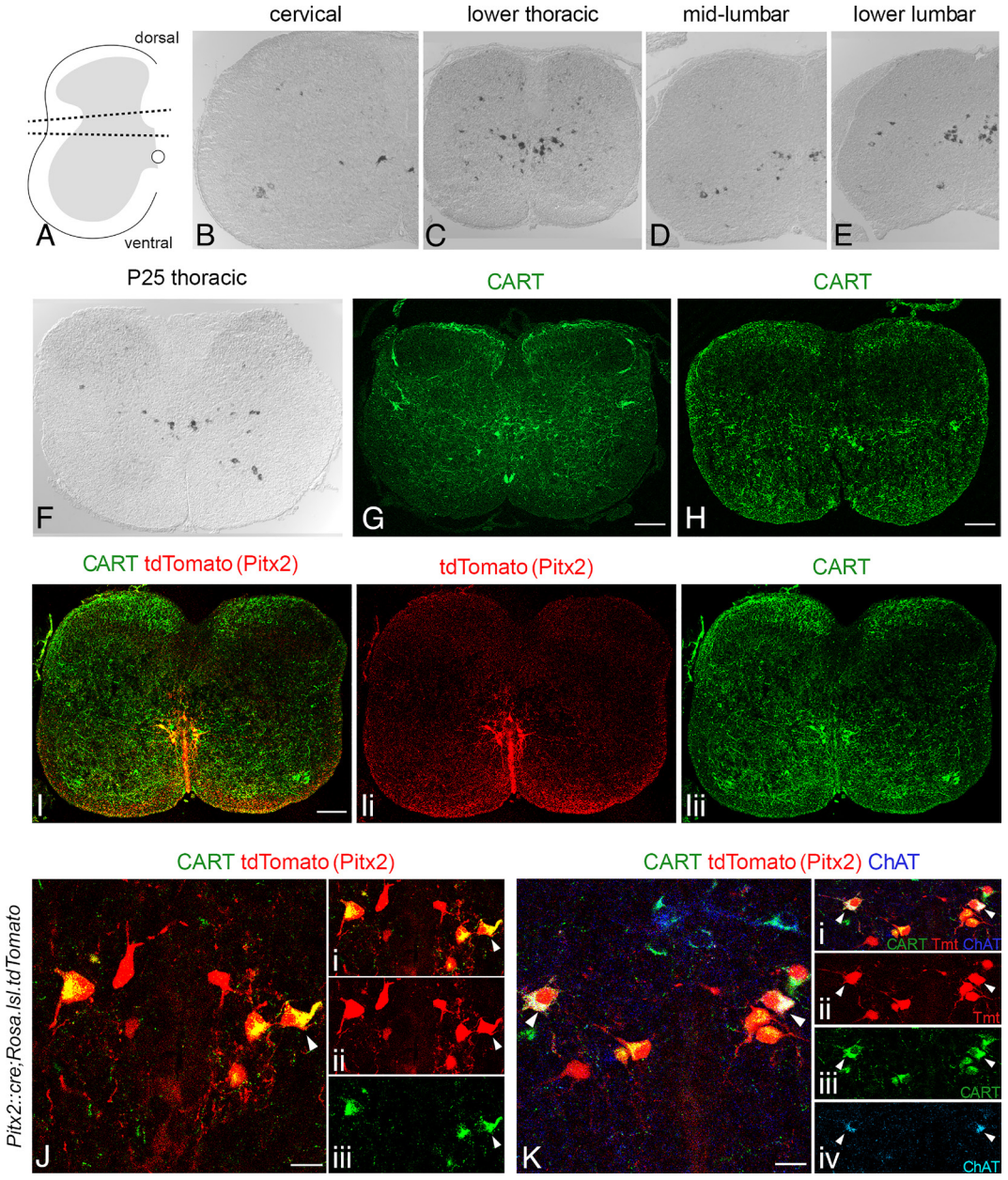

Fig. 1. CART and Pitx2 expression in the spinal cord partially overlap. (*A*) Schematic representation of the tissue dissected for the ventral vs. dorsal horn microarray screen. Tissue between dotted lines was discarded. (*B–E*) *Cart* mRNA detection in all levels of P8 mouse spinal cord as revealed by in situ hybridization. (*F*) *Cart* mRNA detection in P25 spinal cord. The presence of *Cart* mRNA is mainly concentrated in the pericentral canal region as well as in some motor neuron somata. (*G* and *H*) CART neuropeptide detection in spinal cord cross sections of P8 (*G*) and P0 mice (*H*). (*I–Iii*) Partial codetection (yellow) of CART (green) and tdTomato (red) in the Pitx2 expressing neurons from spinal cords of *Pitx2::Cre*;*Rosa.lsl.tdTomato* mice (P0). (*J*, *Ji* and *Jiii*) High magnification of the pericentral canal region (*J*), cropped neurons presented in separate panels [merge-*Ji*, tdTomato (red)-*Jii*, CART (green)-*Jiii*]. Some tdTomato+ neurons coexpress CART (tdTomato+/CART+ neurons), only one is indicated by a white arrowhead for simplicity; tdTomato+/CART− neurons are also observed (P0). (*K–Kiv*). V0c cholinergic neurons coexpress CART (tdTomato+/ChAT+/CART+, red/blue/green, respectively, white arrowheads, *K*). Cropped neurons presented in separate panels [merge-*Ki*, tdTomato (red)-*Kii*, CART (green)-*Kiii*, ChAT (Cyan)-*Kiv*]. Noncholinergic (V0g) Pitx2 neurons can be subdivided into CART expressing (tdTomato+/CART+/ChAT−, red and green) and non expressing (tdTomato+/CART−/ChAT−, red only) (P0). [Scale bars, 100 μm (*G–I*), 20μm (*J* and *K*).]

recruitment and FR, which are two key mechanisms for the gradation of muscle force.

Previous work has reported higher densities of C boutons on fast compared to slow-type motor neurons (29), in addition to differences in the postsynaptic structures located at C bouton synapses that contact different types of motor neurons (30, 31). We therefore investigated whether CART or acetylcholine-mediated modulation of the intrinsic properties that shape the recruitment or FR of motor neurons varied for fast vs. slow-type motor neurons from animals aged P7 to P12. Motor neuron subtypes were identified based on their repetitive firing profiles (32, 33) with fast motor neurons identified by a delayed firing and accelerating FR (Fig. 3*Ai*; n = 21) and slow motor neurons identified by an immediate onset of repetitive firing and steady or adapting FR (Fig. 3*Aii*; n = 16). Consistent with these two populations representing fast and slow motor neuron types, and in line with previous work (32, 33), delayed firing motor neurons had a lower input resistance (Fig. 3*Aiii*; t(33)= 4.7, P = 4.3e-5) and a higher rheobase (Fig. 3*Aiii*; t(34) = 4.96, P = 2.1e-5), along with other differentiating intrinsic properties (summarized in *SI Appendix*, Fig. S6).

Having confirmed techniques to physiologically distinguish fast vs. slow-type motor neurons, we next investigated the effects of CART (1 μM) or muscarine (10 μM) on the intrinsic properties

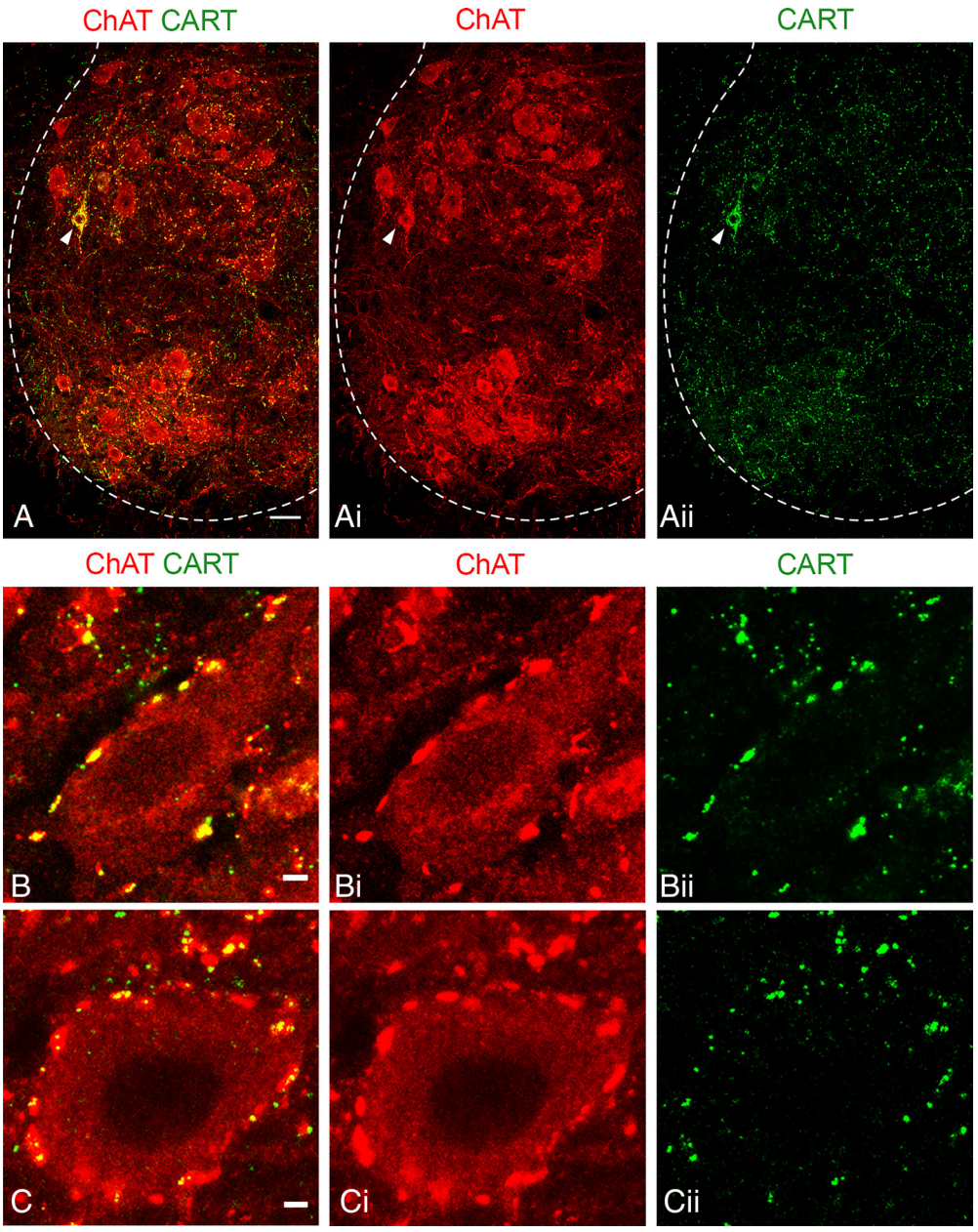

Fig. 2. CART detection in C bouton synapses and in a subset of spinal motor neurons. (*A*, *Ai* and *Aii*) Immunohistochemistry in P25 mice with antibodies against ChAT (red) and CART (green) reveals the presence of CART puncta in the motor neuron area, specifically on motor neuron membranes. CART immunoreactivity is also observed in a few motor neuron somata (white arrowhead). (Scale bar, 20 μm.) (*B*, *Bi* and *Bii*) Colocalization of ChAT (red) and CART (green) in the cholinergic C bouton synapses on motor neurons of P8 mice. (*C*, *Ci* and *Cii*) C bouton synapses of P25 mice also contain CART. (Scale bars, 2 μm (*B* and *C*).]

of these motor neuron subtypes (L1 - L6 spinal segments). Interestingly, both CART and muscarine selectively modulated several intrinsic properties in fast motor neurons only. Specifically, CART hyperpolarized the resting membrane potential (RMP) (Fig. 3 *Bi*, *Bii*, and *Ci*; F (1.6,29) = 19.7, p = 2.2e-5) and increased the input resistance (Fig. 3*Cii*; F (1.6, 30.6) = 7.6, P = 0.003), which translated to a reduction in the recruitment current (Fig. 3 *Di* and *Diii*; F (1.6, 30.6) = 3.5, P = 0.05), in fast- but not slow-type motor neurons (Fig. 3 *Di* and *Diii*). In a subset of experiments (n = 5), we applied CART in the presence of TTX and reproduced the increase in input resistance and hyperpolarization of RMP in fast motor neurons (*SI Appendix*, Fig. S7). The decrease in recruitment current of the largest fast motor neurons led to an increase in the recruitment gain across the motor pool (Fig. 3*Div*). Consistent with previous reports (28, 34), we found that muscarine had a range of effects on motor neuron intrinsic properties. However, these effects were most robust in fast-type motor neurons (n = 12), with no significant changes in the slow-type motor neurons (n = 7). In the fast motor neurons, muscarine depolarized the RMP (Fig. 3 *Bi*, *Bii*, and *Ci*: F (1.7,15.3) = 13.9, P = 5.4e-4), but did not change the input resistance (Fig. 3*Cii*) or recruitment current (Fig. 3 *Ei–Eiv*).

Both CART and muscarine also produced complementary modulation of fast but not slow motor neuron FR, assessed during slow depolarizing current ramps. CART increased FR at the lower end of the frequency current range (minimum FR: Fig. 4 *Ai* and *Bi*; F (1.9,31.2) = 6.6, P = 0.005) and FR at 2× recruitment (Fig. 4*Bii*; F (1.8,29.7) = 3.4, P = 0.04), with no change in maximal FR (Fig. 4*Biii*; F (1.8,29.8) = 1.2, P = 0.3) in fast but not slow motor neurons (Fig. 4 *Aii* and *Bi–Biii*). In contrast to CART, muscarine did not change the FR at recruitment (Fig. 4 *Ai* and *Bi*; F (1.3,12.7) = 1.8, P = 0.2) but did

Table 1. Distribution of CART immunoreactivity patterns

Distribution of CART immunoreactivity patterns in the C boutons synapse in different ages

	Age groups				
Patterns	P10	P25	8 to 9 wk	6 mo	1 y old
Compact	7.2%	9.3%	6.8%	7.8%	14.7%
Puncta along the synapse	15.4%	16.7%	23.1%	29.4%	24.1%
1–3 puncta	31.6%	30.9%	27.6%	26.4%	27.2%
Peripheral puncta	19.2%	12.5%	11.7%	18.4%	19.6%
No CART	26.6%	30.6%	30.8%	18%	14.4%

In the P10, P25, 8 to 9 wk, 6 mo old, 1-y-old age groups (n = 3 mice per age group), a mean of 544 synapses per motor neuron (1,208 µm optical section thickness) were evaluated in lumbar segments (14 µm slices). The percentage of CART+ C bouton synapses differs depending on age.

increase the FR at 2× recruitment (Fig. 4*Bii*: F (1.4,13.2) = 9.2, P = 0.006) and the maximal FR (Fig. 4*Biii*: F (0.9,7.8) = 7.6, P = 0.03) in fast but not slow motor neurons (Fig. 4 *Aii* and *Bi–Biii*). Both action potential rise time and half-width were unaltered by CART or muscarine (*SI Appendix*, Tables S1 and S2). CART and muscarine produced opposing control of the medium afterhyperpolarization (mAHP). CART increased the amplitude (Fig. 4 *Ci* and *Di*; F (1.2, 20.4) = 12.9, P = 0.001) and half-width (Fig. 4*Dii*; F (1.6, 27.1) = 5.3, P = 0.02) of the mAHP of fast but not slow motor neurons (Fig. 4 *Cii*, *Di*, and *Dii*). Muscarine reduced the mAHP amplitude (Fig. 4 *Ciii* and *Di*: F (1.6,13.7) = 19.7, P = 2.3e-4) and half-width (Fig. 4*Dii*; F (1.6,13.7) = 10.7, P = 0.002) in fast but not slow motor neurons (Fig. 4 *Civ*, *Di*, and *Dii*). The electrophysiological responses of motor neurons to CART did not differ between males and females or across spinal segments (*SI Appendix*, Fig. S8).

Together, these data indicate that CART indeed affects motor neuron excitability. The two neurotransmitters, CART and acetylcholine, increase motor output through differential control of motor neuron subtypes via two key mechanisms that are important for the gradation of muscle force, with CART increasing recruitment and FR at the lower end of the input range and acetylcholine increasing FR throughout much of the input range without affecting recruitment or FR at recruitment.

CART and Acetylcholine Are Not Essential for the Formation and Maintenance of C Bouton Structure. Having identified CART as a unique signaling molecule that is present alongside acetylcholine at C bouton synapses, we next set out to determine the relative importance of the two signaling pathways and what roles, if any, they may play in supporting the structural integrity of C bouton synapses (Fig. 5 *A–Q*). To address this, we studied C bouton synapses in P25 mice, identified with antibodies against vAChT and ChAT, when CART was globally knocked out (35) or ChAT conditionally deleted from V0c interneurons and their efferent C boutons (*Dbx1::Cre;ChAT*$^{fl/fl}$), (36–38). As expected, we detected no immunoreactivity for the CART peptide in *CART*$^{KO/KO}$ mice (Fig. 5*C*). Strikingly, despite the absence of CART, C bouton synapses on motor neuron somata (ChAT+) remained well formed and appeared morphologically unaltered as confirmed by both ChAT (Fig. 5*Cii*) and vAChT immunoreactivity (Fig. 5*Ciii*). This result suggests that despite the complete absence of CART peptide, C bouton terminals remain structurally intact and develop in a manner consistent with control mice (Fig. 5 *A–Aiii*). The assessment of the conditional elimination of the ChAT gene from V0c interneurons yielded similar results (Fig. 5 *E–Eiii*). Despite the absence of the ChAT enzyme (Fig. 5*Eii*), CART peptide was still detected (Fig. 5*Ei*) in C bouton synapses as revealed by vAChT labeling (Fig. 5*Eiii*), suggesting that C bouton gross anatomy remains intact, and that CART peptide expression is unaltered and independent of the presence of acetylcholine (schematic representations Fig. 5 *B*, *D*, and *F*).

We next considered the possibility that CART and acetylcholine may serve parallel roles in supporting C bouton synapses, such that the deletion of one could support synapse integrity in the absence of the other. We therefore examined C boutons in double knockout mice (KO), with both global KO of CART and V0c-selective deletion of ChAT (*Dbx1::Cre;ChAT*$^{fl/fl}$*;CART*$^{KO/KO}$, double KO) (*SI Appendix*, Fig. S9). However, examination of the C bouton synapses on the somata of motor neurons of double KO mice using the cholinergic marker vAChT revealed that the C boutons remain detectable despite the absence of ChAT and CART (Fig. 5 *G–Jiii*). No difference was observed in the number of vAChT+ C boutons in double KO mice compared to WT (Mann–Whitney U = 1,867, P = 0.6730 two-tailed; Fig. 5*O* and *SI Appendix*, Table S3) nor in the size of vAChT+ terminals (Mann–Whitney U = 25,733, P = 0.0666 two-tailed; *SI Appendix*, Table S4).

We also considered the possibility that deletion of CART and ChAT could influence the clustering of the key receptor expressed on the postsynaptic membrane at C bouton synapses. We therefore examined the postsynaptic M2 receptors (Fig. 5 *K–Niii*). We found no difference in either the total number of M2 receptor clusters on motor neuron somata (Mann-Whitney U = 1,001, P = 0.4402 two-tailed; Fig. 5*P* and *SI Appendix*, Table S3) nor in the size of M2 receptor clusters (Mann-Whitney U = 25658, P = 0.0537 two-tailed; *SI Appendix*, Table S4). The number of M2 receptor clusters aligned with vAChT+ boutons also remained unaltered in double KO mice compared to wildtype controls (Mann–Whitney U = 963, P = 0.2880 two-tailed; Fig. 5*Q* and *SI Appendix*, Table S3). Together, these data suggest that neither CART nor acetylcholine is essential for the maintenance of the pre- and postsynaptic structure of C boutons, given that we find no change in C bouton number, gross synapse morphology and size, or postsynaptic organization and M2 cluster size in double KO mice with V0c specific deletion of ChAT and global CART KO.

CART and Acetylcholine Are Critical Signaling Molecules for Vigorous Motor Behaviors. Given that CART is expressed at C boutons and provides amplification of motor neuron output in parallel with acetylcholine-mediated signaling, we next set out to determine whether perturbing CART or acetylcholine signaling at C boutons could influence motor behaviors that require greater levels of strength and muscle coordination. We deployed a hanging wire test, which requires mice to recruit multiple muscle groups of the torso and limbs, providing a useful tool to evaluate possible impairments in high muscle force exertion, and coordination. In this task, mice are positioned on

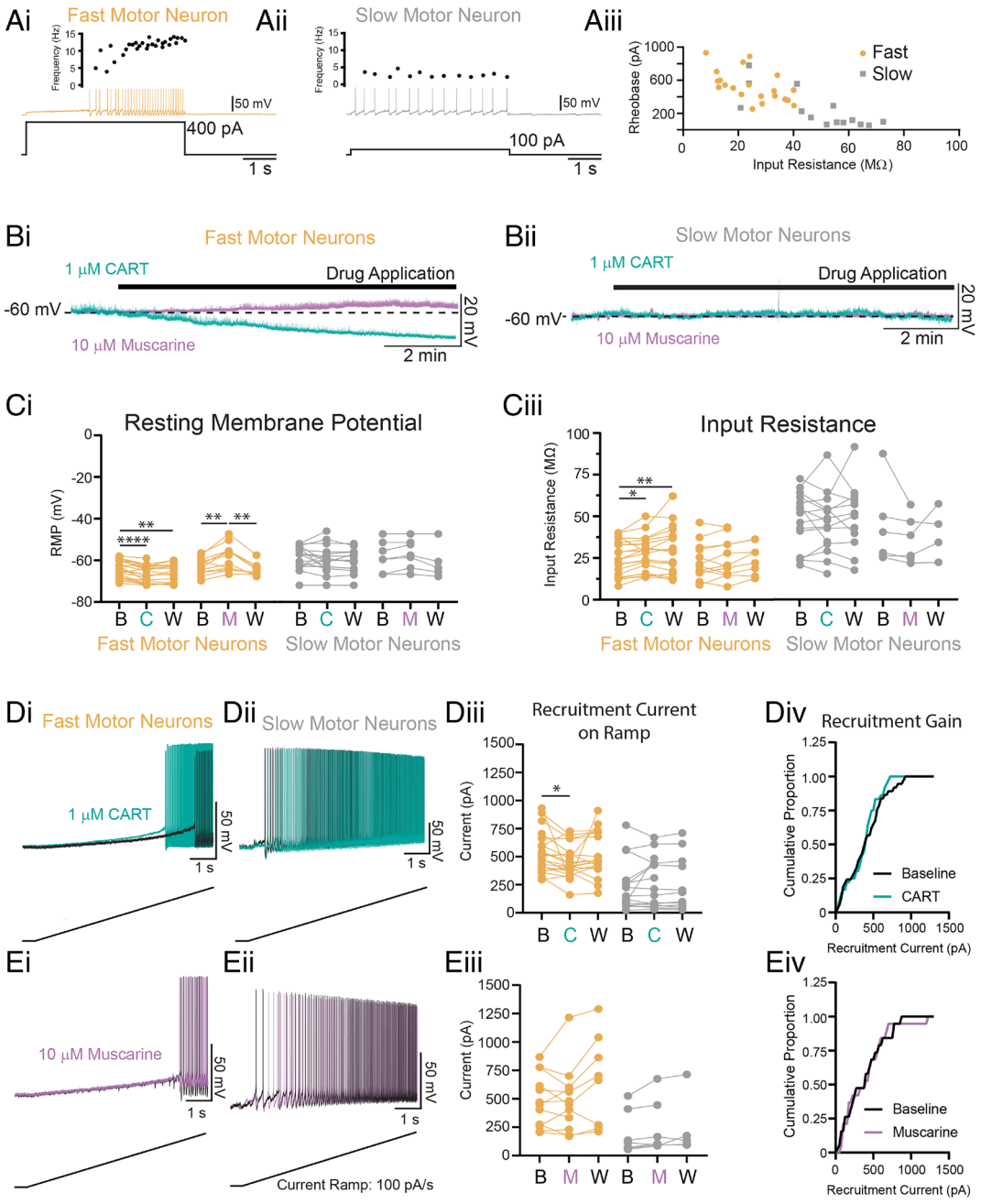

Fig. 3. CART but not muscarine facilitates the recruitment of fast but not slow-type motor neurons. (*Ai* and *Aii*) Representative trace of fast (*Ai*: orange) and slow (*Aii*: gray) motor neurons identified with whole-cell patch-clamp electrophysiology. (*Aiii*) Scatter plot of input resistance and recruitment current (rheobase) demonstrate that fast motor neurons have a high rheobase and low input resistance, whereas slow-firing motor neurons have relatively low rheobase and high input resistance. (*Bi* and *Bii*) Representative traces depicting the effects of CART (1 μM; green) and muscarine (10 μM; purple) on the membrane potential of fast (*Bi*) and slow (*Bii*) motor neurons. (*Ci*) CART (C) and muscarine (M) produce opposing effects on the resting membrane potential (RMP) of fast (orange) motor neurons but do not alter the RMP of slow (gray) motor neurons. (*Cii*) CART (C) increases the input resistance of fast (orange) but not slow (gray) motor neurons. Muscarine (M) does not affect input resistance of fast or slow motor neurons. (*Di* and *Dii*) Representative trace of the subthreshold voltage trajectory and onset of repetitive firing during a slow depolarizing current ramp (applied at 100 pA/s) in fast (*Di*) and slow (*Dii*) motor neurons both before (black traces) and after application of 1 μM CART (green traces). (*Diii*) CART significantly reduces the recruitment current in fast (orange) but not slow motor neurons (gray). (*Div*) Cumulative proportion histogram of motor neuron recruitment currents depicts an increase in the recruitment gain of the sample of motor neurons studied before (black) and after CART (green). (*Ei* and *Eii*) Representative trace of the subthreshold voltage trajectory and onset of repetitive firing in fast (*Ei*) and slow (*Eii*) motor neurons both before (black traces) and after application of 10 μM muscarine (purple traces). (*Eiii*) Muscarine did not alter the recruitment current in fast (orange) or slow motor neurons (grey) and did not change the recruitment gain (*Eiv*). All measurement were made at baseline (B), following drug application [CART (C), muscarine (M)], and following a wash period with regular aCSF (W). Asterisks denote significance (*$P < 0.05$, **$P < 0.01$, ***$P < 0.001$. ****$P < 0.0001$) from Holm-Sidak post hoc following 2 factor (Repeated measures) ANOVA.

an elevated wire from which they hang with all four limbs. The number of times that animals reached the end of the hanging wire, during a 3-min period, was counted as an indirect measure of muscle strength and endurance (39–41). Motor performance on this task was assessed in mice with global CART KO, C bouton-specific deletion of ChAT, or both manipulations in tandem (double KO).

Adult mice that had ChAT deleted from C boutons (*Dbx1::Cre;ChAT$^{fl/fl}$*, n = 22, mean ± SEM = 4.59 ± 0.65) exhibited a significant decrease in the number of times they reached the end

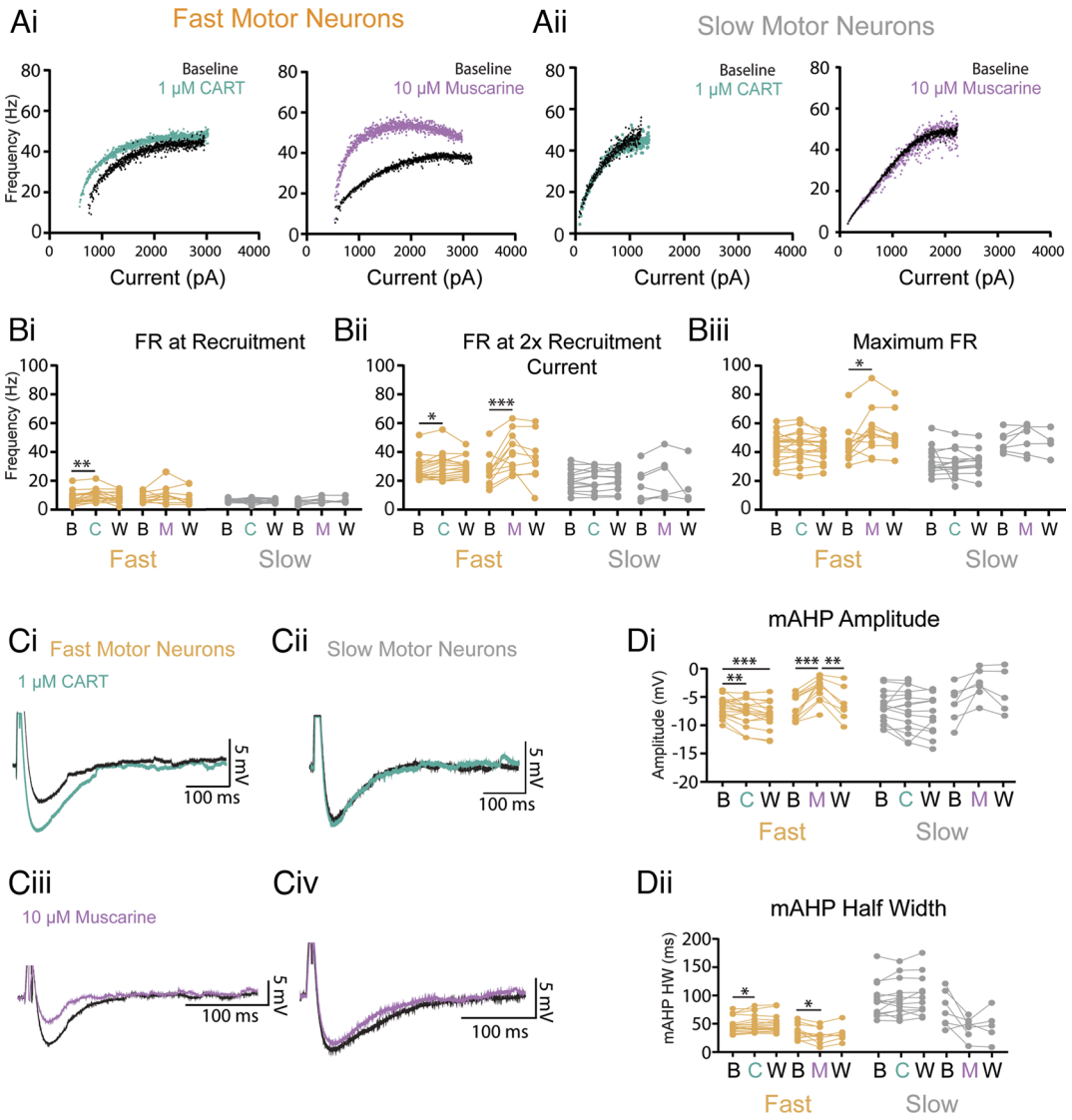

Fig. 4. CART and muscarine modulate distinct components of frequency–current relationship and produce opposing control of mAHP in fast but not slow-type motor neurons. (*Ai*) Representative frequency–current plots depicting changes in FR during a slow (100 pA/s) depolarizing current ramp for fast motor neurons before (black) and after CART (green) or muscarine (purple). (*Aii*) Representative frequency–current plots depicting FR on current ramp for slow motor neurons before (black) and after CART (green) or muscarine (purple). (*Bi–Biii*) Effect of CART and muscarine on FR at recruitment, 2× recruitment current, and maximum. (*Bi*) CART significantly increases the FR of fast but not slow motor neurons at recruitment (minimum FR) and 2 times recruitment current (*Bii*) but does not alter maximal FR (*Biii*), whereas muscarine does not alter FR for fast motor neurons at recruitment (*Bi*), but does increase FR at 2 times recruitment current (*Bii*) and maximal FR (*Biii*). Neither CART nor muscarine alter FR of slow motor neurons. (*Ci* and *Cii*) Representative trace of the mAHP in fast (*Ci*) and slow (*Cii*) motor neurons both before (black traces) and after application of 1 μM CART (green traces). (*Ciii* and *Civ*) Representative trace of the mAHP in fast (*Ciii*) and slow (*Civ*) motor neurons both before (black traces) and after application muscarine (purple traces). (*Di*) CART significantly increases, whereas muscarine decreases the amplitude of the mAHP in fast motor neurons. Neither CART, nor muscarine, alter the mAHP amplitude of slow motor neurons. (*Dii*). CART significantly increases, whereas muscarine (M) decreases the half-width (HW) of the mAHP in fast motor neurons but do not alter the mAHP HW of slow motor neurons. All measurements were made at baseline (B), following drug application [CART (C), muscarine (M)], and following a wash period with regular aCSF (W). Asterisks denote significance (*$P < 0.05$, **$P < 0.01$, ***$P < 0.001$. ****$P < 0.0001$) from Holm-Sidak post hoc following 2 factor (Repeated measures) ANOVA.

of the wire compared to control mice ($ChAT^{fl/fl}$ mice, n = 23, mean ± SEM = 7.09 ± 0.90; t(43) = −2.28, $P = 0.031$). Data from male and female mice were combined as there were no significant differences between sexes in *Dbx1::Cre;ChAT* $^{fl/fl}$ mice (n = 11, mean ± SEM = 5.09 ± 1.11 for female and n = 11, mean ± SEM = 4.09 ± 0.72 for male mice, t(20) = 0.757, $P = 0.459$) or $ChAT^{fl/fl}$ mice (n = 13, mean ± SEM = 6.46 ± 0.91 for female and n = 10, mean ± SEM = 7.9 ± 1.73 for male mice t(21) = 0.785, $P = 0.441$). This result indicates that motor performance related to strength is diminished when mice have the ChAT gene exclusively eliminated in V0c interneurons (Fig. 6*A*). Consistent with animals that had ChAT eliminated from C boutons ($Dbx1::Cre;ChAT^{fl/fl}$), CART KO mice ($CART^{KO/KO}$, n =17, mean ± SEM = 5.76 ± 0.70) also reached the end of the wire significantly fewer times compared to wild type control mice (n = 11, mean ± SEM = 9.27 ± 1.04, t(26) = −2.89, $P = 0.008$), providing strong evidence of a behavioral deficit in the CART KO mice; however, this effect was specific to males only (Fig. 6*B*). The female CART KO mice (n = 16, mean ± SEM = 9.94 ± 1.56) did not differ significantly in the number of reaches from their wild type counterparts, (n = 11, mean ± SEM = 7.55 ± 1.57, t(25) = 1.04, $P = 0.307$), (Fig. 6*C*). Data from male and female mice were not combined as there was a significant difference between male and female $CART^{KO/KO}$ mice (n = 16, mean ± SEM = 9.94 ± 1.56 for female and n = 17, mean ± SEM = 5.76 ± 0.7 for male mice, t(20.92) = −2.44, $P = 0.024$). A similar, significant decrease in the number of times the end of the wire was reached was found in male mice lacking both CART globally and ChAT exclusively from V0c interneurons ($Dbx1::Cre;ChAT^{fl/fl};CART^{KO/KO}$, n = 21, mean ± SEM

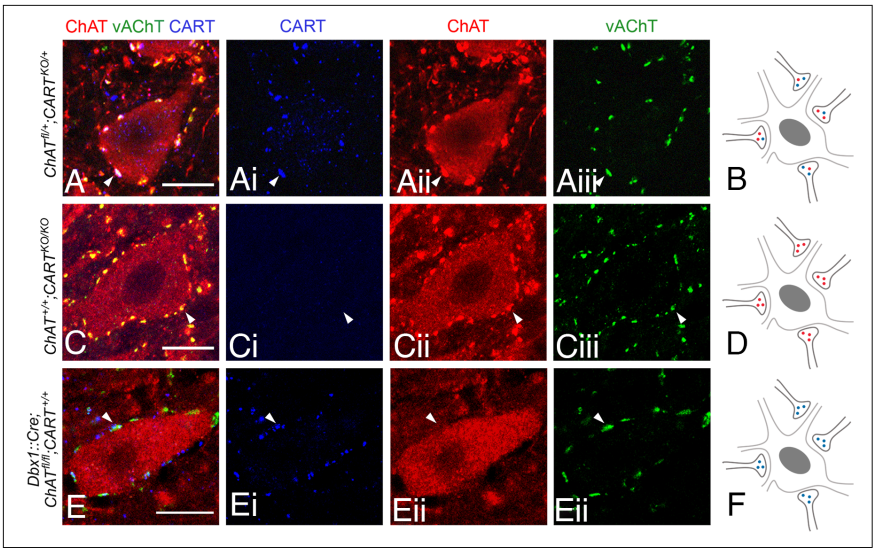

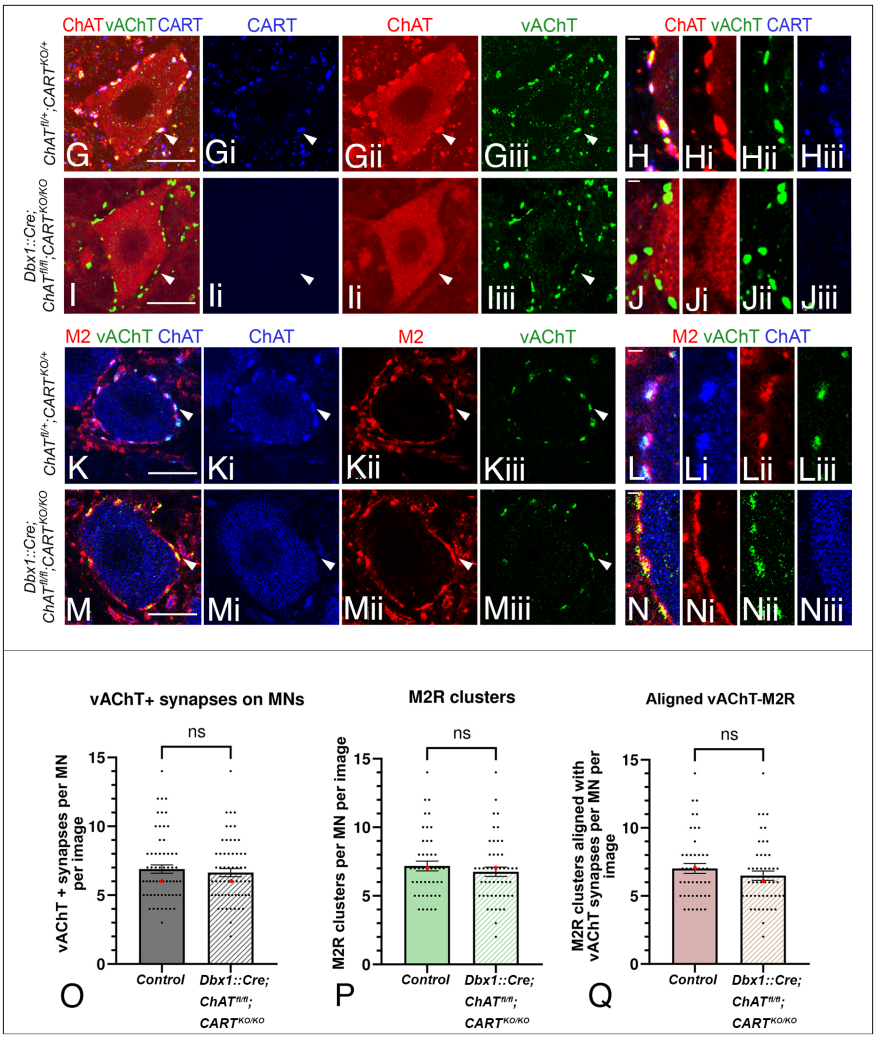

Fig. 5. Gross anatomy of C boutons remains unchanged after genetic elimination of CART and ChAT from the synapse. (*A–Aiii*) C boutons on somata of motor neurons of wild-type mice are marked by CART (blue) and the cholinergic markers ChAT (red) and vAChT (green). (*B*) Schematic representation of a motor neuron receiving C boutons containing acetylcholine (red) and CART (blue). (*C–Ciii*) ChAT (red) and vAChT (green) expression are not disrupted in C boutons of $CART^{KO/KO}$ mice. (*D*) Schematic representation of a motor neuron receiving C boutons containing acetylcholine (red) only. (*E–Eiii*) CART (blue) and vAChT (green) expression are not disrupted following the genetic deletion of ChAT in V0c interneurons. (*F*) Schematic representation of a motor neuron receiving C boutons containing CART (blue) only. (*G–Giii*) CART (blue), ChAT (red), and vAChT (green) are present in C boutons of herterozygous $ChAT^{fl/+};CART^{KO/+}$ mice. The white arrowhead points to one representative triple-positive C bouton. (*H–Hiii*) High-magnification image showing the colocalization of CART (blue), ChAT (red), and vAChT (green) in individual C boutons. (*I–Iiii*) Despite the conditional knockout of *ChAT* and the complete knockout of *Cart* in $Dbx1::Cre;ChAT^{fl/fl};CART^{KO/KO}$ mice, the presynaptic components of C boutons remain intact, as evident by the presence of vAChT (green). The white arrowhead points to one CART−/ChAT− C bouton that expresses vAChT. (*J–Jiii*) High-magnification image showing the presence of vAChT (green) in individual C boutons that lack both ChAT and CART. (*K–Kiii*) The ChAT+/vAChT+ C boutons (blue and green respectively) on motor neurons of control $ChAT^{fl/+};CART^{KO/+}$ mice are in close apposition to M2 muscarinic receptor clusters (red). The white arrowhead points to a ChAT+/M2+/vAChT+ C bouton. (*L–Liii*) High-magnification image showing the alignment of the postsynaptic M2 muscarinic receptor (red) with the ChAT+/vAChT+ presynaptic part of the synapse (red and green respectively). (*M–Miii*) Postsynaptic clustering of M2 receptors (red) with presynaptic vAChT (green) is unaltered in $Dbx1::Cre;ChAT^{fl/fl};CART^{KO/KO}$ double KO mice. The white arrowhead points to a vAChT+/M2+ synapse. (*N–Niii*) High-magnification image showing the alignment of M2 postsynaptic muscarinic receptors (red) with the vAChT+ (green) C boutons in $Dbx1^{cre/+};ChAT^{fl/fl};CART^{KO/KO}$ mice. (*O–Q*) No change was observed in the number of vAChT+ terminals ($P = 0.6730$, two-tailed), M2 muscarinic receptor clusters ($P = 0.4402$, two-tailed) or their alignment ($P = 0.2880$, two-tailed) despite the simultaneous elimination of ChAT and CART in C boutons. The bar charts represent the mean number of synapses per motor neuron with superimposed data points representing the data distribution. Data are presented as mean values (±SEM) and were combined from different sexes as no sex-dependent differences were observed. The median is also presented as a red dot superimposed in each graph. For panels *O–Q* "image" corresponds to optical thickness of 1,208 µm. [Scale bars, 20 µm, (*A–M*), 1 µm (*H–N*).]

= 3.9 ± 0.50) compared to control mice (n = 28, mean ± SEM = 5.68 ± 0.57, t(47) = −2.25, $P = 0.029$), (Fig. 6*D*) suggesting a sex-specific motor deficit for this particular genotype. The female counterparts ($Dbx1::Cre;ChAT^{fl/fl};CART^{KO/KO}$, n = 15, mean ± SEM = 6.33 ± 0.98) did not differ significantly compared to control mice (n = 25, mean ± SEM = 6.16 ± 0.58, t(38) = 0.163, $P = 0.872$), (Fig. 6 *E* and *F*). Data from male and female mice were not combined as there was a significant difference between male and female $Dbx1::Cre;ChAT^{fl/fl};CART^{KO/KO}$ mice (n = 15, mean ± SEM = 6.33 ± 0.98 for female and n = 21, mean ± SEM = 3.90 ± 0.49 for male mice, t(34) = −2.39, $P = 0.023$).

Together, these results indicate that CART and acetylcholine exhibit parallel roles in the control of motor behavior, with a particular role for CART in male mice.

Discussion

Spinal circuits composed of distributed populations of interneurons support a diverse array of functions including the control of movement. Much of what we have learned about roles for spinal interneurons for the control of movement has been derived from the study of locomotor movements that can be broken into properties related to the rhythm and pattern (2, 42, 43). However, complex behaviors are critically dependent on the ability to fine-tune the degree of precision and vigor of the underlying movements. Here, we describe new mechanisms by which V0c interneurons and their C bouton synapses facilitate motor output to increase movement vigor.

Our previous work identified a subset of spinal cholinergic interneurons, called V0c interneurons that are defined by the expression of the transcription factor Pitx2, and constitute the sole source of C bouton synapses on motor neurons. The C bouton synapse is believed to be an important neuromodulatory synapse that task-dependently increases motor output in mammals (12, 16). Presynaptic components of C boutons (V0c terminals) include cholinergic markers ChAT and vAChT, (44, 45) along with Synaptobrevin (Vamp2) (46), ErbB2/4 receptors (47), P2X7R purinergic receptors, and possibly Nicotinic Acetylcholine Receptors (48, 49). The postsynaptic membrane aligned with C bouton terminals houses N-type calcium channels (50), Ca2+-dependent-K+ channels (SK2/3) (31), calcium-activated chloride channels (30), and ErbB3/4 receptors (51). In the Subsurface Cisterns of C boutons, Sigma-1 receptors (52), connexin32 (53, 54), indole-N-methyl transferase (52), and Neuregulin 1 (55) have been identified. The wide range of proteins localized to pre- and postsynaptic regions of C boutons points toward a particularly complicated multicomponent synapse. Here, we have demonstrated further complexity to this synapse, by revealing a neuropeptide, encoded by the *Cart* gene, in V0c interneurons at all levels of the spinal cord and in the vast majority of the cholinergic C bouton synapses on motor neurons. These initial anatomical data led us to investigate whether CART may provide a novel complementary signaling mechanism at this important neuromodulatory synapse.

CART was first described in the rat striatum as a hyper-expressed mRNA after cocaine and amphetamine administration (56). Since then, CART has been detected throughout the CNS and has been linked to multiple functions, such as olfaction and vision (24, 57) pain processing (24, 58, 59), addictive behavior (60, 61), regulation of appetite, and body weight (35, 62, 63) as well as stress responses and anxiety (64–66). In the spinal cord, CART has been previously traced in fibers in laminae I and II of the dorsal horn, in some somata in laminae X and VII, and in SPNs (24, 25, 67).

The fact that we detected CART in synapses on motor neurons raised the question of its involvement in motor control. KO of CART exerted functional consequences and led to a poorer performance on the hanging wire test, a motor task that requires increased muscle strength and endurance, pointing to an important role in motor control (Fig. 6*B*). Surprisingly, this deficit was only observed in males. This finding is perhaps not entirely unexpected, given that sex differences regarding CART expression during a stressful and demanding motor task have been previously observed (68). Also, changes have been observed in C boutons, specifically in males, during disease (69–71). Although there are currently limited tools (conditional KO mice, agonists, antagonists) available to study CART's specific role in motor control, it is possible that this behavioral deficit might be due to the loss of CART in other areas of the CNS. For example, hypothalamic circuits that involve CART signaling, related to motivation and reward, could affect the overall performance. Moreover, we cannot exclude that the lack of CART from the CART+ proportion of V0g neurons could also play a role in the motor deficits observed in our behavioral task. However, this is unlikely since we find no direct connections from V0g interneurons to motor neurons (12). Our in vitro electrophysiological analyses provided evidence that CART influences spinal circuits. Here, we show that CART and acetylcholine provide differential control of motor neuron subtypes that innervate different muscle fibers; with a bias toward motor neuron subtypes that innervate high-force generating, fast-twitch muscle fibers that are generally recruited during tasks that require increased levels of muscle force (*SI Appendix*, Fig. S10 *A–D*). Interestingly, CART and acetylcholine accomplish this control through distinct yet parallel physiological mechanisms for the gradation of muscle force with CART decreasing the recruitment current and the acetylcholine agonist muscarine increasing FR across much of the frequency current range. While differential control of motor neuron subtypes that innervate axial muscles has been described in zebrafish (72, 73), this is the first demonstration that multiple neuromodulators released from the same synapse on hindlimb motor neurons can produce complementary control through distinct, but parallel mechanisms. Based on our interdisciplinary approach, we can now correlate these single-cell mechanisms to changes in animal behavior, since we observed that lack of CART in male mice leads to poorer motor performance. It remains to be determined whether peptidergic cotransmission involving CART is a common feature of other cholinergic modulatory systems that regulate the output neurons of a range of neural networks (18–20).

The postsynaptic receptors and target ion channels that mediate CART and acetylcholine's differential control of motor neuron subtypes are not yet known. However, differences in ion channels that control the recruitment and FR of fast and slow motor neurons are beginning to be described and could contribute to their differential modulation (31, 33). For example, monoamines including 5HT and norepinephrine have been shown to augment motor neuron firing by activating sodium and calcium channels that conduct persistent inward currents (6–10). 5HT fibers are present at the distal dendrites (74) and the axon initial segment (75) of motor neurons where the sodium and calcium channels that conduct persistent inward currents are distributed (76–79). 5HT fibers are also found around V0c interneurons (12). Given our new work, it is possible that 5HT could indirectly facilitate motor neuron output through these inputs to V0c interneurons. While it has not yet been shown whether 5HT can modulate the excitability of V0c interneurons, one could speculate that serotonergic modulation of V0c interneurons could work in parallel with cholinergic and CART signaling at somato-dendritic compartments to facilitate motor neuron output.

The intrinsic properties of hindlimb motor neurons studied both in vitro and in vivo have not been found to differ between sexes (33, 80). However, sex differences in human motor unit function are beginning to be described (81–84), lending the possibility that sex differences in motor function may arise from a divergence in their neuromodulatory control. In support of this notion, we found specific deficits in motor function in male mice, which is in line with previous anatomical studies that report greater C bouton innervation of fast compared to slow motor neurons in male mice (71). In contrast to behavioral analyses conducted in adult animals, we did not detect any sex differences in the effects of CART on spinal motor neurons in postnatal mice, which is consistent with anatomical studies at similar developmental stages (69). Although C boutons can modulate spinal motor output as early as the first postnatal week (16), they undergo considerable maturation of their molecular composition through the first and second postnatal weeks (50), which occurs in parallel to changes in cholinergic modulation of motor neurons during this time (34, 85). Testosterone has been

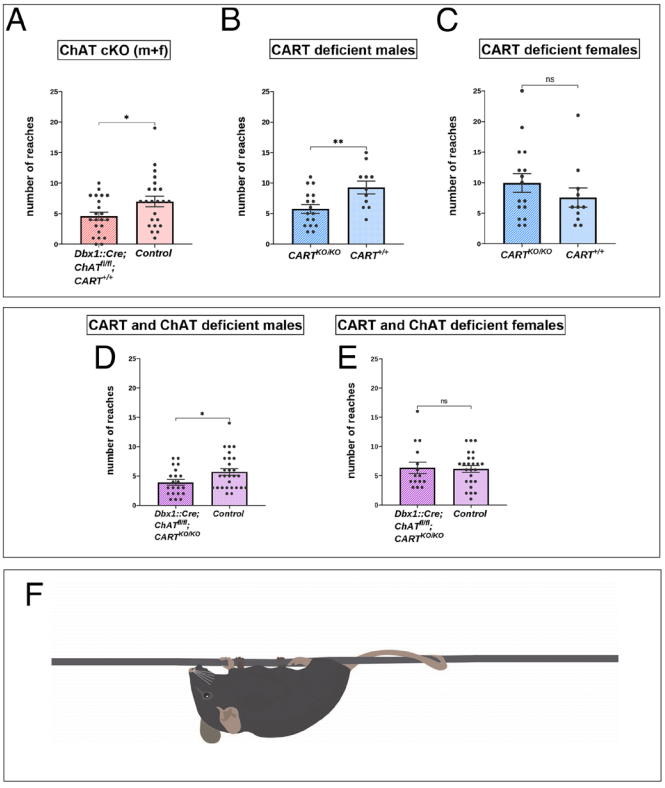

Fig. 6. Behavioral effects of the complete KO of the *Cart* gene and the conditional KO of the *ChAT* gene in C boutons. Hanging wire test analysis (reaches method) for monitoring muscle strength in mice lacking ChAT in C boutons or CART or of both. Muscle strength is reflected by the number of times that each mouse reaches the end of the wire trying to escape after being positioned to suspend from the middle of a 55cm long wire (reaches). (*A*) *Dbx1:Cre;ChAT*$^{fl/fl}$ mice (males and females combined) performed significantly fewer reaches than the control *ChAT*$^{fl/fl}$ littermates (P = 0.031, two-tailed). (*B*) *CART KO* male mice performed significantly fewer reaches than the *CART*$^{+/+}$ male mice (P = 0.008, two-tailed). (*C*) There were no significant differences between the *CART KO* female mice and the *CART*$^{+/+}$ female mice in the number of reaches performed (P = 0.307, two-tailed). (*D*) *Dbx1::Cre;ChAT*$^{fl/fl}$*;CART*$^{KO/KO}$ male mice performed significantly fewer reaches than the control male mice (P = 0.029, two-tailed). (*E*) There were no significant differences between the *Dbx1::Cre;ChAT*$^{fl/fl}$*;CART*$^{KO/KO}$ female mice and the control female mice in the number of reaches performed (P = 0.872, two-tailed). Data are expressed as mean (±SEM). *P < 0.05, **P < 0.01. (*F*) Illustration of the mice in the starting position of the hanging wire test suspended by all four limbs from the middle of the wire in the behavioral apparatus.

demonstrated to influence the number and size of synapses on motor neurons (86, 87); therefore, it is possible that sex differences in neuromodulatory control of motor neurons may emerge at stages later than the second postnatal. Regarding CART receptors, recent studies have pinpointed the G-Protein-Coupled-Receptor (GPCR) Gpr160 as a putative receptor for the CART peptide, proposing that CARTp/Gpr160 signaling in the dorsal horn of the spinal cord mediates neuropathic pain through a c-fos and ERK/CREB pathway (88). Furthermore, CARTp/Gpr160 coupling in the rat brainstem has been proven necessary for the anorexigenic and antidipsogenic effects of exogenous CART administration (89). The identity of the CART peptide receptor in the ventral horn and in particular in the motor neuron membrane remains to be determined; however, its discovery will have the potential to reveal the intracellular signaling mechanisms initiated by CART-motor neuron communication.

C bouton source neurons (Pitx2+ and CART+), the V0c interneurons, were traditionally believed to increase motor output by releasing acetylcholine that acts on M2 muscarinic receptors. Given that chemogenetic activation of V0c interneurons produced only a subset of the effects exerted by global pharmacological activation of muscarinic receptors (16, 28, 34), it has been suggested that C boutons produce a distinct set of cholinergic modulatory actions on motor output, with other effects produced by additional, as yet undefined, cholinergic inputs. However, here we show that CART replicates a subset of the effects of chemogenetic activation of V0c interneurons that are not elicited through pharmacological activation of muscarinic receptors, which includes decreased rheobase, increased input resistance, and increased mAHP amplitude. This result suggests that the CART and acetylcholine may provide comodulation of motor neurons at C boutons synapses. The diversity in modulatory actions between studies could be accounted for by distinct control of fast and slow motor neuron subtypes, which is only beginning to be studied. The diversity in CART function, apart from the recipient motor neuron, is also reflected in the diverse CART expression profiles at C bouton synapses, which were previously believed to be a homogenous synapse. CART is found in most C boutons in different patterns, all of which could be observed throughout the animals' lifespan (Table 1). In line with our observations, diversity in synapse nanostructure, arising from different inputs, has been reported to also change in ventral vs. dorsal areas, during development and through adulthood (90). Further, V0c interneuron diversity can also be accounted for by ipsilaterally and bilaterally projecting populations (91). C bouton diversity is further supported by the demonstration that V0c interneurons subdivide into connexin36 positive and negative subpopulations (92). This gap junction protein is also differentially distributed in C boutons, with fast motor neurons having a greater abundance of connexin 36+ terminals than slow motor neurons. Thus, even within a small subset of functionally defined spinal interneurons, the V0c subset, we find that there is marked diversity with respect to their anatomy and function depending on source neurons, target motor neuron subtypes, and also sex. This highlights perhaps unexpected but marked diversity in a prominent neuromodulatory synapse, the C bouton synapse, that was once believed to be homogeneous.

The diversity of synaptic components in C bouton synapses, in conjunction with our findings of their functional role, reveals a highly complex and specified component of the motor circuit with a well-defined purpose. Strikingly, we find that the establishment of the V0c-motor neuron synaptic contacts, which are regulated by signals during development, seems to be oblivious of the neurotransmitter content of the C boutons, since the genetic elimination of CART, acetylcholine, or both, did not seem to affect the presence or alter the anatomy of the C bouton synapse nor of its pre- and postsynaptic components. This finding lays the groundwork for the investigation of the wiring of interneuronal motor circuits during development and the elucidation of the importance of functional output for target selection and structural stability of synapses during ontogeny.

In conclusion, we have identified CART neuropeptide together with acetylcholine in the C bouton synapse on motor neurons and propose a unique role for CART at these synapses, which is important for the neural control of movement. CART facilitates recruitment and FR at the lower end of the input range of fast-type motor neurons, while acetylcholine augments maximal FR throughout most of the input range of fast-type motor neurons. Thus, differential neuromodulatory control via acetylcholine and CART may serve as a means to more effectively fine-tune muscle activation and force generation and may act in parallel to the descending monoaminergic input. This unique mechanism for adjusting the gain of motor output may be applicable to cholinergic modulatory systems throughout the CNS.

Materials and Methods

Detailed information on material and methods used in this study are found in *SI Appendix*.

Mouse Lines. The following mouse lines were used for experiments: *Pitx2::Cre* (26), *Rosa.stop.tdTomato* (27), *Dbx1::Cre* (36), *ChAT$^{fl/fl}$* (37, 38), *CART$^{KO/KO}$* (35), all maintained on a C57/Bl6 background, along with wild-type mice. All experiments were approved by the respective animal welfare authorities. The sex of the animal was considered in all experiments and data were analyzed accordingly where sex-dependent differences were present. Individuals of ages from P0 to 4 to 6 mo old were used, with the respective ages being mentioned in the relevant results sections.

Immunohistochemistry and Imaging. Intact spinal cords were isolated via ventral vertebrectomy from perfused animals. All Immunohistochemistry experiments were performed in spinal cord cryo-sections of 15 to 20 μm. Sections were washed and incubated in primary and then secondary-fluorescent antibodies, before being observed under the confocal microscope.

Electrophysiology and Pharmacology. Experiments were performed on male and female wild-type C57 BlJ/6 mice from postnatal days 7 to 12 (n = 30). Whole-cell patch-clamp recordings were obtained from motor neurons of rostral and caudal lumbar segments, in slice preparations. Motor neurons were identified based on location in the ventrolateral region with somata greater than 20 μm. Fast and slow motor neurons were identified as by refs. 32 and 93 based on the onset latency at repetitive firing threshold using a 5-s square depolarizing current at rheobase. Working concentrations of 1 μM CART and 10 μM muscarine were used for in vitro experiments.

Behavioral Test. The hanging wire test (reaches method) (Van Putten, 2011 DMD_M.2.1.004) was utilized to assess limb and trunk muscle strength of mice.

Data, Materials, and Software Availability. All data are included in the manuscript and supporting information.

ACKNOWLEDGMENTS. We would like to acknowledge the following people for their contributions to this manuscript: Dr. Niels Wierup for kindly providing us with the *CART$^{KO/KO}$* mouse line, Eirini Eleftheriadi for helping with the graphic design in illustrations of the figures, Despoina Bosveli for further analyzing part of the anatomy data, Dr. Nikolaos Kostomitsopoulos for advice and support at the BRFAA mouse facility, and Dr. David L. McLean, Dr. Katharina Quinlan, and Dr. Stamatis N. Pagakis for critically reading the manuscript. We would also like to thank BRFAA Imaging Unit personnel for support on imaging. This work was supported by the General Secretariat for Research and Technology (ARISTEIA II 4257, L.Z.), Fondation SANTE (L.Z.), a Marie Curie Re-Integration Grant (268323, L.Z.), the Hellenic Foundation for Research and Innovation (spinMNALS, 4013, L.Z.) and by a St. Andrews Restarting Research Fund (S.A.S. and G.B.M.). S.A.S. was funded by a Royal Society Newton International Fellowship (NIF/R1/180091) and a Natural Sciences and Engineering Research Council of Canada (NSERC) Postdoctoral Fellowship (NSERC-PDF-517295-2018) and M.M. by the National Scholarship Foundation (IKY).

Author affiliations: [a]Center of Basic Research, Biomedical Research Foundation Academy of Athens, Athens 11527, Greece; and [b]School of Psychology and Neuroscience, University of St. Andrews, St. Andrews KY16 9JP, United Kingdom

1. S. Gosgnach *et al.*, Delineating the diversity of spinal interneurons in locomotor circuits. *J. Neurosci.* **37**, 10835–10841 (2017).
2. M. Goulding, Circuits controlling vertebrate locomotion: Moving in a new direction. *Nat. Rev. Neurosci.* **10**, 507–518 (2009).
3. E. Henneman, Relation between size of neurons and their susceptibility to discharge. *Science* **126**, 1345–1347 (1957).
4. R. E. Burke, D. N. Levine, P. Tsairis, F. E. Zajac, Physiological types and histochemical profiles in motor units of the cat gastrocnemius. *J. Physiol.* **234**, 723–748 (1973).
5. H. S. Milner-Brown, R. B. Stein, R. Yemm, Changes in firing rate of human motor units during linearly changing voluntary contractions. *J. Physiol.* **230**, 371 (1973).
6. J. Hounsgaard, I. Mintz, Calcium conductance and firing properties of spinal motoneurones in the turtle. *J. Physiol.* **398**, 591–603 (1988).
7. J. Hounsgaard, O. Kiehn, Ca++ dependent bistability induced by serotonin in spinal motoneurons *Exp. Brain Res.* **57**, 422–425 (1985).
8. R. H. Lee, C. J. Heckman, Enhancement of bistability in spinal motoneurons in vivo by the noradrenergic α1 agonist methoxamine. *J. Neurophysiol.* **81**, 2164–2174 (1999).
9. J. françois Perrier, J. Hounsgaard, 5-HT2 receptors promote plateau potentials in turtle spinal motoneurons by facilitating an L-type calcium current. *J. Neurophysiol.* **89**, 954–959 (2003).
10. P. J. Harvey, X. Li, Y. Li, D. J. Bennett, 5-HT2 receptor activation facilitates a persistent sodium current and repetitive firing in spinal motoneurons of rats with and without chronic spinal cord injury. *J. Neurophysiol.* **96**, 1158–1170 (2006).
11. S. Conradi, S. Skoglund, Observations on the ultrastructure of the initial motor axon segment and dorsal root boutons on the motoneurons in the lumbosacral spinal cord of the cat during postnatal development. *Acta Physiol. Scand. Suppl.* **333**, 53–76 (1969).
12. L. Zagoraiou *et al.*, A cluster of cholinergic premotor interneurons modulates mouse locomotor activity. *Neuron* **64**, 645–662 (2009).
13. G. M. Lanuza, S. Gosgnach, A. Pierani, T. M. Jessell, M. Goulding, Genetic identification of spinal interneurons that coordinate left-right locomotor activity necessary for walking movements. *Neuron* **42**, 375–386 (2004).
14. A. Pierani *et al.*, Control of interneuron fate in the developing spinal cord by the progenitor homeodomain protein Dbx1. *Neuron* **29**, 367–384 (2001).
15. L. Moran-Rivard *et al.*, Evx1 is a postmitotic determinant of V0 interneuron identity in the spinal cord. *Neuron* **29**, 385–399 (2001).
16. F. Nascimento *et al.*, Synaptic mechanisms underlying modulation of locomotor-related motoneuron output by premotor cholinergic interneurons. *Elife* **9**, e54170 (2020).
17. H. P. Clamann, Motor unit recruitment and the gradation of muscle force. *Phys. Ther.* **73**, 830–843 (1993).
18. C. Xiao *et al.*, Cholinergic mesopontine signals govern locomotion and reward through dissociable midbrain pathways. *Neuron* **90**, 333–347 (2016).
19. J. Pickford, R. Apps, Z. I. Bashir, Muscarinic receptor modulation of the cerebellar interpositus nucleus in vitro. *Neurochem. Res.* **44**, 627–635 (2019).
20. Y. Li, E. Hollis, Basal forebrain cholinergic neurons selectively drive coordinated motor learning in mice. *J. Neurosci.* **41**, 10148–10160 (2021).
21. O. Kiehn, S. J. B. Butt, Physiological, anatomical and genetic identification of CPG neurons in the developing mammalian spinal cord. *Prog. Neurobiol.* **70**, 347–361 (2003).
22. K. J. Dougherty *et al.*, Locomotor rhythm generation linked to the output of spinal Shox2 excitatory interneurons. *Neuron* **80**, 920–933 (2013).
23. N. M. Fenwick, C. L. Martin, I. J. Llewellyn-Smith, Immunoreactivity for cocaine- and amphetamine-regulated transcript in rat sympathetic preganglionic neurons projecting to sympathetic ganglia and the adrenal medulla. *J. Comp. Neurol.* **495**, 422–433 (2006).
24. E. O. Koylu, R. Couceyro, P. D. Lambert, M. J. Kuhar, Cocaine-and amphetamine-regulated transcript peptide immunohistochemical localization in the rat brain. *J. Comp. Neurol.* **391**, 115–132 (1998).
25. S. L. Dun, D. A. Chianca, N. J. Dun, J. Yang, J. K. Chang, Differential expression of cocaine- and amphetamine-regulated transcript-immunoreactivity in the rat spinal preganglionic nuclei. *Neurosci. Lett.* **294**, 143–146 (2000).
26. W. Liu, J. Selever, M. F. Lu, J. F. Martin, Genetic dissection of Pitx2 in craniofacial development uncovers new functions in branchial arch morphogenes, late aspects of tooth morphogenesis and cell migration. *Development* **130**, 6375–6385 (2003).
27. L. Madisen *et al.*, A robust and high-throughput Cre reporting and characterization system for the whole mouse brain. *Nat. Neurosci.* **13**, 133–140 (2009).
28. G. B. Miles, R. Hartley, A. J. Todd, R. M. Brownstone, Spinal cholinergic interneurons regulate the excitability of motoneurons during locomotion. *Proc. Natl. Acad. Sci. U.S.A.* **104**, 2448–2453 (2007).
29. J. Hellström, A. L. R. Oliveira, B. Meister, S. Cullheim, Large cholinergic nerve terminals on subsets of motoneurons and their relation to muscarinic receptor type 2. *J. Comp. Neurol.* **460**, 476–486 (2003).
30. C. Soulard *et al.*, Spinal motoneuron TMEM16F acts at c-boutons to modulate motor resistance and contributes to ALS pathogenesis. *Cell Rep.* **30**, 2581–2593.e7 (2020).
31. A. S. Deardorff *et al.*, Expression of postsynaptic Ca^{2+} -activated K^+ (SK) channels at C-bouton synapses in mammalian lumbar α-motoneurons. *J. Physiol.* **591**, 875–897 (2013).
32. F. Leroy, B. Lamotte d'Incamps, R. D. Imhoff-Manuel, D. Zytnicki, Early intrinsic hyperexcitability does not contribute to motoneuron degeneration in amyotrophic lateral sclerosis. *Elife* **3**, e04046 (2014).
33. S. A. Sharples, G. B. Miles, Maturation of persistent and hyperpolarization-activated inward currents shapes the differential activation of motoneuron subtypes during postnatal development. *Elife* **10**, e71385 (2021).
34. F. Nascimento, L. R. B. Spindler, G. B. Miles, Balanced cholinergic modulation of spinal locomotor circuits via M2 and M3 muscarinic receptors. *Sci. Rep.* **9**, 14051 (2019).
35. N. Wierup *et al.*, CART knock out mice have impaired insulin secretion and glucose intolerance, altered beta cell morphology and increased body weight. *Regul. Pept.* **129**, 203–211 (2005).
36. F. Bielle *et al.*, Multiple origins of Cajal-Retzius cells at the borders of the developing pallium. *Nat. Neurosci.* **8**, 1002–1012 (2005).
37. T. Misgeld *et al.*, Roles of neurotransmitter in synapse formation: Development of neuromuscular junctions lacking choline acetyltransferase. *Neuron* **36**, 635–648 (2002).
38. M. Buffelli *et al.*, Genetic evidence that relative synaptic efficacy biases the outcome of synaptic competition. *Nature* **424**, 430–434 (2003).
39. P. Kundu *et al.*, Integrated analysis of behavioral, epigenetic, and gut microbiome analyses in AppNL-G-F, AppNL-F, and wild type mice. *Sci. Rep.* **11**, 1–20 (2021).
40. M. Luna-Sánchez *et al.*, The clinical heterogeneity of coenzyme Q10 deficiency results from genotypic differences in the Coq9 gene. *EMBO Mol. Med.* **7**, 670–687 (2015).
41. S. F. Martinez-Huenchullan *et al.*, Utility and reliability of non-invasive muscle function tests in high-fat-fed mice. *Exp. Physiol.* **102**, 773–778 (2017).
42. S. Grillner, A. El Manira, Current principles of motor control, with special reference to vertebrate locomotion. *Physiol. Rev.* **100**, 271–320 (2020).
43. O. Kiehn, Decoding the organization of spinal circuits that control locomotion. *Nat. Rev. Neurosci.* **17**, 224–238 (2016).
44. M. Connaughton, J. V. Priestley, M. V. Sofroniew, F. Eckenstein, A. C. Cuello, Inputs to motoneurones in the hypoglossal nucleus of the rat: Light and electron microscopic immunocytochemistry for choline acetyltransferase, substance P and enkephalins using monoclonal antibodies. *Neuroscience* **17**, 205–224 (1986).
45. D. Nachmansohn, A. L. Machado, The formation of acetylcholine. A new enzyme: "Choline acetylase". *J. Neurophysiol.* **6**, 397–403 (1943).

46. J. Hellström, U. Arvidsson, R. Elde, S. Cullheim, B. Meister, Differential expression of nerve terminal protein isoforms in VAChT-containing varicosities of the spinal cord ventral horn. *J. Comp. Neurol.* **411**, 578–590 (1999).
47. A. Casanovas *et al.*, Neuregulin 1–ErbB module in C-bouton synapses on somatic motor neurons: Molecular compartmentation and response to peripheral nerve injury. *Sci. Rep.* **7**, 1–17 (2017).
48. Z. Deng, R. E. W. Fyffe, Expression of P2X7 receptor immunoreactivity in distinct subsets of synaptic terminals in the ventral horn of rat lumbar spinal cord. *Brain Res.* **1020**, 53–61 (2004).
49. I. Khan *et al.*, Nicotinic acetylcholine receptor distribution in relation to spinal neurotransmission pathways. *J. Comp. Neurol.* **467**, 44–59 (2003).
50. J. M. Wilson, J. Rempel, R. M. Brownstone, Postnatal development of cholinergic synapses on mouse spinal motoneurons. *J. Comp. Neurol.* **474**, 13–23 (2004).
51. J. Lasiene *et al.*, Neuregulin 1 confers neuroprotection in SOD1-linked amyotrophic lateral sclerosis mice via restoration of C-boutons of spinal motor neurons. *Acta Neuropathol. Commun.* **4**, 15 (2016).
52. T. A. Mavlyutov *et al.*, Development of the sigma-1 receptor in C-terminals of motoneurons and colocalization with the N, N′-dimethyltryptamine forming enzyme, indole-N-methyl transferase. *Neuroscience* **206**, 60–68 (2012).
53. J. I. Nagy, T. Yamamoto, L. M. Jordan, Evidence for the cholinergic nature of C-terminals associated with subsurface cisterns in alpha-motoneurons of rat. *Synapse* **15**, 17–32 (1993).
54. N. Zampieri, T. M. Jessell, A. J. Murray, Mapping sensory circuits by anterograde transsynaptic transfer of recombinant rabies virus. *Neuron* **81**, 766–778 (2014).
55. X. Gallart-Palau *et al.*, Neuregulin-1 is concentrated in the postsynaptic subsurface cistern of C-bouton inputs to α-motoneurons and altered during motoneuron diseases. *FASEB J.* **28**, 3618–3632 (2014).
56. J. Douglass, A. A. McKinzie, P. Couceyro, PCR differential display identifies a rat brain mRNA that is transcriptionally regulated by cocaine and amphetamine. *J. Neurosci.* **15**, 2471–2481 (1995).
57. P. R. Couceyro, E. O. Koylu, M. J. Kuhar, Further studies on the anatomical distribution of CART by in situ hybridization. *J. Chem. Neuroanat.* **12**, 229–241 (1997).
58. M. Imad Damaj, J. Zheng, B. R. Martin, M. J. Kuhar, Intrathecal CART (55–102) attenuates hyperlagesia and allodynia in a mouse model of neuropathic but not inflammatory pain. *Peptides (N.Y.)* **27**, 2019–2023 (2006).
59. M. Ohsawa, S. L. Dun, L. F. Tseng, J. K. Chang, N. J. Dun, Decrease of hindpaw withdrawal latency by cocaine- and amphetamine-regulated transcript peptide to the mouse spinal cord. *Eur. J. Pharmacol.* **399**, 165–169 (2000).
60. J. N. Jaworski, A. Vicentic, R. G. Hunter, H. L. Kimmel, M. J. Kuhar, CART peptides are modulators of mesolimbic dopamine and psychostimulants. *Life Sci.* **73**, 741–747 (2003).
61. F. W. Lohoff *et al.*, Genetic variants in the cocaine- and amphetamine-regulated transcript gene (CARTPT) and cocaine dependence. *Neurosci. Lett.* **440**, 280–283 (2008).
62. G. De Lartigue *et al.*, Cocaine- and amphetamine-regulated transcript mediates the actions of cholecystokinin on rat vagal afferent neurons. *Gastroenterology* **138**, 1479–1490 (2010).
63. S. Ludvigsen, L. Thim, A. M. Blom, B. S. Wulff, Solution structure of the satiety factor, CART, reveals new functionality of a well-known fold. *Biochemistry* **40**, 9082–9088 (2001).
64. E. O. Koylu, B. Balkan, M. J. Kuhar, S. Pogun, Cocaine and amphetamine regulated transcript (CART) and the stress response. *Peptides (N.Y.)* **27**, 1956–1969 (2006).
65. S. M. Smith *et al.*, Cocaine- and amphetamine-regulated transcript activates the hypothalamic-pituitary-adrenal axis through a corticotropin-releasing factor receptor-dependent mechanism. *Endocrinology* **145**, 5202–5209 (2004).
66. M. P. Dandekar *et al.*, Importance of cocaine- and amphetamine-regulated transcript peptide in the central nucleus of amygdala in anxiogenic responses induced by ethanol withdrawal. *Neuropsychopharmacology* **33**, 1127–1136 (2008).
67. S. L. Dun, Y. K. Ng, G. C. Brailoiu, E. A. Ling, N. J. Dun, Cocaine- and amphetamine-regulated transcript peptide-immunoreactivity in adrenergic C1 neurons projecting to the intermediolateral cell column of the rat. *J. Chem. Neuroanat.* **23**, 123–132 (2002).
68. B. Balkan *et al.*, CART expression in limbic regions of rat brain following forced swim stress: Sex differences. *Neuropeptides* **40**, 185–193 (2006).
69. L. R. Herron, G. B. Miles, Gender-specific perturbations in modulatory inputs to motoneurons in a mouse model of amyotrophic lateral sclerosis. *Neuroscience* **226**, 313–323 (2012).
70. T. L. Wells, J. R. Myles, T. Akay, C-boutons and their influence on amyotrophic lateral sclerosis disease progression. *J. Neurosci.* **41**, 8088–8101 (2021).
71. A. N. Bak *et al.*, Cytoplasmic TDP-43 accumulation drives changes in C-bouton number and size in a mouse model of sporadic Amyotrophic Lateral Sclerosis. *Mol. Cell Neurosci.* **125**, 103840 (2022).
72. M. Bertuzzi, K. Ampatzis, Spinal cholinergic interneurons differentially control motoneuron excitability and alter the locomotor network operational range. *Sci. Rep.* **18**, 1–10 (2018).
73. U. Jha, V. Thirumalai, Neuromodulatory selection of motor neuron recruitment patterns in a visuomotor behavior increases speed. *Curr. Biol.* **30**, 788–801.e3 (2020).
74. S. J. Montague *et al.*, Nonuniform distribution of contacts from noradrenergic and serotonergic boutons on the dendrites of cat splenius motoneurons. *J. Comp. Neurol.* **521**, 638–656 (2013).
75. A. S. Deardorff, S. H. Romer, R. E. W. Fyffe, Location, location, location: The organization and roles of potassium channels in mammalian motoneurons. *J. Physiol.* **599**, 1391–1420 (2021).
76. K. P. Carlin, K. E. Jones, Z. Jiang, L. M. Jordan, R. M. Brownstone, Dendritic L-type calcium currents in mouse spinal motoneurons: Implications for bistability. *Eur. J. Neurosci.* **12**, 1635–1646 (2000).
77. S. M. ElBasiouny, D. J. Bennett, V. K. Mushahwar, Simulation of dendritic Cav1.3 channels in cat lumbar motoneurons: Spatial distribution. *J. Neurophysiol.* **94**, 3961–3974 (2005).
78. C. Brocard *et al.*, Cleavage of Na+ channels by calpain increases persistent Na+ current and promotes spasticity after spinal cord injury. *Nat. Med.* **22**, 404–411 (2016).
79. H. S. Jørgensen *et al.*, Increased axon initial segment length results in increased Na+ currents in spinal motoneurones at symptom onset in the G127X SOD1 mouse model of amyotrophic lateral sclerosis. *Neuroscience* **468**, 247–264 (2021).
80. H. Drzymała-Celichowska, J. Celichowski, M. Bączyk, P. Krutki, The electrophysiological properties of hindlimb motoneurons do not differ between male and female rats. *Eur. J. Neurosci.* **56**, 4176–4186 (2022).
81. J. G. Inglis, D. A. Gabriel, Sex differences in motor unit discharge rates at maximal and submaximal levels of force output. *Appl. Physiol. Nutrition Metab.* **45**, 1197–1207 (2020).
82. Y. Guo *et al.*, Neuromuscular recruitment strategies of the vastus lateralis according to sex. *Acta Physiol. (Oxf.)* **235**, 13803 (2022).
83. C. A. Taylor, B. H. Kopicko, F. Negro, C. K. Thompson, Sex differences in the detection of motor unit action potentials identified using high-density surface electromyography. *J. Electromyograp. Kinesiol.* **65**, 102675 (2022).
84. S. T. Jenz *et al.*, Estimates of persistent inward currents in lower limb motoneurons are larger in females than males. *J. Neurophysiol.* **129**, 1322–1333 (2023), 10.1152/JN.00043.2023 (22 May 2023).
85. C. C. Smith, R. M. Brownstone, Kv2 conductances are not required for C-bouton mediated enhancement of motoneuron output. bioRxiv [Preprint] (2022). https://doi.org/10.1101/2022.07.23.501232 (Accessed 1 June 2023).
86. A. Matsumoto, P. E. Micevych, A. P. Arnold, Androgen regulates synaptic input to motoneurons of the adult rat spinal cord. *J. Neurosci.* **8**, 4168–4176 (1988).
87. A. Matsumoto, Androgen stimulates neuronal plasticity in the perineal motoneurons of aged male rats. *J. Comp. Neurol* **430**, 389–395 (2001).
88. G. L. C. Yosten *et al.*, GPR160 de-orphanization reveals critical roles in neuropathic pain in rodents. *J. Clin. Invest.* **130**, 2587 (2020).
89. C. J. Haddock *et al.*, Signaling in rat brainstem via Gpr160 is required for the anorexigenic and antidipsogenic actions of cocaine- and amphetamine-regulated transcript peptide. **320**, R236–R249 (2021), 10.1152/ajpregu.00096.2020.
90. M. J. Broadhead *et al.*, Nanostructural diversity of synapses in the mammalian spinal cord. *Sci. Rep.* **10**, 8180 (2020).
91. A. E. Stepien, M. Tripodi, S. Arber, Monosynaptic rabies virus reveals premotor network organization and synaptic specificity of cholinergic partition cells. *Neuron* **68**, 456–472 (2010).
92. A. J. Recabal-Beyer, J. M. M. Senecal, J. E. M. Senecal, B. D. Lynn, J. I. Nagy, On the organization of connexin36 expression in electrically coupled cholinergic V0c neurons (partition cells) in the spinal cord and their C-terminal innervation of motoneurons. *Neuroscience* **485**, 91–115 (2022).
93. F. Leroy, B. L. d'Incamps, D. Zytnicki, Potassium currents dynamically set the recruitment and firing properties of F-type motoneurons in neonatal mice. *J. Neurophysiol.* **114**, 1963–1973 (2015).